Supporting Information

A Two-in-One Probe: Imaging Lipid Droplets and Endoplasmic Reticulum in Tandem

Shabnam Mansuri[a], Paramasivam Mahalingavelar[b], Virupakshi Soppina[c]* and Sriram Kanvah[a]*

[a]Department of Chemistry, Indian Institute of Technology Gandhinagar, Palaj, Gandhinagar, Gujarat – 382055: Email: sriram@iitgn.ac.in

[b]School of Chemistry and Biochemistry and School of Materials Science and Engineering Georgia Institute of Technology, Atlanta, Georgia 30332

[c]Department of Biological Engineering, Indian Institute of Technology Gandhinagar, Palaj, Gandhinagar, Gujarat -382055 Email: vsoppina@gmail.com

Supplementary Information Contents

S1. Synthetic procedures and characterization

7-Diethylamino-coumarin (1a)[1]:

Diethyl malonate (1.18 mL, 7.755 mmol) and 4-(diethylamino)-2-hydroxybenzaldehyde **1** (1 g, 5.17 mmol) were dissolved in absolute ethyl alcohol (100 mL), and then piperidine (1 mL) was added stepwise under ice bath. Under N_2, the reaction mixture was refluxed at 80 °C for 12 h. After evaporating solvent in vacuum, 40 mL of concentrated HCl/glacial acetic acid (1:1, v/v) was added into the reaction mixture. The reaction solution was continued to stir for 48 h at 120 °C. After cooling to room temperature, the resulting mixture was poured into 100 mL of water and neutralized with sodium hydroxide solution (40%) until the pH to 7. The off-white precipitate was filtered and recrystallized from toluene to obtain 1.1 g (97%) of 7-diethylamino-coumarin-**1a**. **^{1}H NMR** (500 MHz, $CDCl_3$, δ): 7.54 (d, *J* = 10 Hz, 1H), 7.25 (d, *J* = 10 Hz, 1H), 6.56 (dd, *J* = 10 Hz, J = 5Hz, 1H), 6.49 (d, 1H), 6.02 (d, *J* = 10 Hz, 1H), 3.40 (q, *J* = 5 Hz, 4H), 1.21 (t, *J* = 5 Hz, 6H). Data is consistent with that previously reported.

***7-(Diethylamino)coumarin-3-carbaldehyde (1b)**:*

Under N_2, freshly distilled anhydrous DMF (5.81 mL, 75.2 mmol) was dropped into $POCl_3$ (3.52 mL, 37.6 mmol) with stirring for 6 h in an ice bath. The solution of 7-diethylamino-coumarin 1a (815.3 mg, 3.76 mmol) in anhydrous 1,2-dichloroethane was added to the above solution, and the mixture was stirred at 80 °C for 12 h. After completing, the mixture was poured into ice water and neutralized with NaOH solution (20%) to pH 7. The formed precipitate was filtered off and washed three times with water. The residue was chromatographed on silica, eluting with petroleum ether/CH_2Cl_2 (2:1, v/v) to form orange solid 1b (726 mg, 79%). **^{1}H NMR** (500 MHz, $CDCl_3$, δ): 10.06 (s, 1H, –CHO), 8.19 (s, 1H), 7.35 (d, *J* = 10.0 Hz, 1H), 6.57 (dd, *J* = 10.0 Hz, 1H), 6.42 (d, 1H), 3.41 (q, *J* = 5 Hz, 4H), 1.19 (t, *J* = 5 Hz, 6H). Data is consistent with that previously reported.

((E)-3-(7-(diethylamino)-2-oxo-2H-chromen-3-yl)-2-(perfluorophenyl)acrylonitrile)* (*PFC):

In a round-bottom flask, **1b** (50 mg, 0.2 mmol) and 2,3,4,5,6-Pentafluorobenzeneacetonitrile (63.3 mg, 0.31 mmol) were mixed in absolute ethanol. To this 0.1 mL of piperidine was added and stirred the mixture at 70 °C for 24 h. This resulted in formation of orange coloured precipitate, which was filtered using suction pump, washed with ethanol, and dried. Yield = 79 mg, 89%, orange solid. **^{1}H NMR** (500 MHz, $CDCl_3$) *δ* (ppm) 8.82 (s, 1H), 7.66 (s, 1H), 7.43 (d, *J* = 10.0 Hz, 1H), 6.65 (dd, *J* = 10.0, 1H), 6.48 (d, *J* = 5 Hz, 1H), 3.48 (q, *J* = 5 Hz, 4H), 1.26 (t, *J* = 5 Hz, 6H)). **^{13}C NMR** (126 MHz, $CDCl_3$) *δ* (ppm) 160.25, 156.41, 151.85, 144.04, 141.43, 130.44, 115.60, 110.96, 109.07, 107.35, 96.13, 91.49, 44.20, 11.46. **^{19}F NMR** (470 MHz, $CDCl_3$) -139.99 (m, 2F), -152.08 (t, 1F), -160.70 (m, 2F). **HR-MS** (ESI-ToF) *m/z*: Calculated for $C_{22}H_{15}F_5N_2O_2$ $[M + H]^+$: 435.1126; Found: 435.1133; error: 0.0007 m/z.

6-bromo-N, N-dimethylnaphthalen-2-amine (2a[2])

In a pressure vessel, a suspension of 6-bromo-2-naphthol **2** (4.00 g, 17.9 mmol), $Na_2S_2O_5$ (6.805 g, 35.8 mmol) and aqueous dimethylamine (40%, 6 mL, 89.5 mmol) in H_2O (40 mL) was left to stir at 145 °C for 4 days. After cooling to room temperature, the reaction mixture was dissolved in CH_2Cl_2 (50 mL). The resulting organic layer was washed with $NaHCO_3$ (5%, 30 mL × 3), dried (Na2SO4), filtered and excess solvent removed. Purification by column chromatography (98:2, Hexane:Ethyl Acetate) afforded the title compound **2a** (4.247 g, 95%, Rf = 0.16) as an off-white solid. **^{1}H NMR** (500 MHz, CDCl3): δ 7.75 (d, J = 1.5 Hz, 1H), 7.53 (d, J = 10 Hz, 1H), 7.44 (d, J = 10 Hz, 1H), 7.34 (dd, J = 10, 5 Hz, 1H), 7.10 (dd, J = 10Hz, 1H), 6.79 (d, J = 5.0 Hz, 1H), 2.97 (s, 6H). Data is consistent with that previously reported

6-(dimethylamino)-2-naphthaldehyde (2b)

A solution of 6-bromo-2-dimethylaminonaphthalene **2a** (500 mg, 1.9988 mmol) in THF (anhydrous, 10 mL) was cooled to -78 °C under nitrogen. To this was added n-BuLi (2.5 M solution in hexane, 0.960 mL, 2.4 mmol) dropwise. After stirring at -78 °C for 2 h, anhydrous DMF (0.77 mL, 10.0 mmol) was slowly added. The reaction was monitored by TLC and after stirring at 0 °C for 10 hours, the reaction mixture was quenched with NH_4Cl (sat., 20 mL). The resulting aqueous phase was then extracted with Et_2O (3 × 20 mL). The combined organic layer was washed with brine (20 mL), dried (Na2SO4), filtered, and the excess solvent was removed. Purification by column chromatography (70:30, Hexane:Ethyl Acetate) afforded the title compound **2b** (378.95 mg, 95%) as a yellow solid. **^{1}H NMR** (500 MHz, CDCl3): δ 9.94 (s, 1H, CHO), 8.08 (s, 1H), 7.76 (dd, J = 10.0 Hz, J= 5.0 Hz, 2H), 7.59 (d, J = 10.0 Hz, 1H), 7.10 (dd, J = 10.0, 5.0 Hz, 1H), 6.81 (d, 1H), 3.06 (s, 6H). Data is consistent with that previously reported.

(E)-3-(6-(dimethylamino)naphthalen-2-yl)-2-(perfluorophenyl)acrylonitrile (PFN)

In a round-bottom flask, **2b** (100 mg, 0.5 mmol) and 2,3,4,5,6-Pentafluorobenzeneacetonitrile (155.325 mg, 0.75 mmol) were mixed in absolute ethanol. To this potassium tert-butoxide (84.165 mg, 0.75 mmol) was added and stirred the mixture at 50 °C for 16 h. This resulted in the formation of a yellow colored precipitate, which was filtered using a suction pump, washed with ethanol, and dried. Yield = 183.63 mg, 94%, yellow solid. **^{1}H NMR** (500 MHz, $CDCl_3$) δ (ppm) 8.13 (s, 1H), 8.05 (d, J = 10 Hz, 1H), 7.75 (d, *J* = 10.0 Hz, 1H), 7.68 (d, *J* = 10.0 Hz, 1H), 7.35 (s, 1H), 7.17 (dd, *J* = 10 Hz, 1H), 6.88 (d, J = 5 Hz, 1H) 3.13 (s, 6H). **^{13}C NMR** (126 MHz, $CDCl_3$) δ (ppm) 152.22, 150.32, 137.04, 132.43, 130.39, 126.88, 125.49, 125.41, 117.02, 116.45, 105.39, 91.30, 40.39**. ^{19}F NMR** (470 MHz, $CDCl_3$) -140.09 (m, 2F), -152.76 (t, 1F), -160.89 (m, 2F). **HR-MS** (ESI-ToF) *m/z*: Calculated for $C_{21}H_{13}F_5N_2$ $[M + H]^+$: 389.1072; Found: 389.1077; error: 0.0005 m/z.

(2E,4E)-5-(4-(dimethylamino)phenyl)-2-(perfluorophenyl)penta-2,4-dienenitrile (PFB)

In a round-bottom flask, 4-(Dimethylamino)cinnamaldehyde 3 (50 mg, 0.3 mmol) and 2,3,4,5,6-Pentafluorobenzeneacetonitrile (93.195 mg, 0.45 mmol) were mixed in 2mL absolute ethanol. To this potassium tert-butoxide (50.5 mg, 0.45 mmol) was added and stirred the mixture at room temperature for 20 h. This resulted in formation of orange coloured precipitate, which was filtered using suction pump, washed with ethanol, and dried. Yield = 97.25 mg, 93%, orange solid. **^{1}H NMR** (500 MHz, $CDCl_3$) δ (ppm) 7.46 (d, J = 10.0 Hz, 1H), 7.26-7.15 (m, 2H), 7.02 (d, *J* = 15.0 Hz, 1H), 6.68 (d, *J* = 10.0 Hz, 1H). **^{13}C NMR** (126 MHz, $CDCl_3$) δ (ppm) 151.86, 150.86, 145.01, 130.31, 128.97, 128.87, 121.85, 119.73, 118.05, 114.96, 110.88, 110.80, 91.30. 39.09. **^{19}F NMR** (470 MHz, $CDCl_3$) -140.27 (m, 2F), -153.50 (t, 1F), -161.19 (m, 2F). **HR-MS** (ESI-ToF) *m/z*: Calculated for $C_{19}H_{13}F_5N_2$ $[M + H]^+$: 365.1072; Found: 365.1079; error: 0.0007 m/z.

S2. Photophysical properties of PFN and PFB

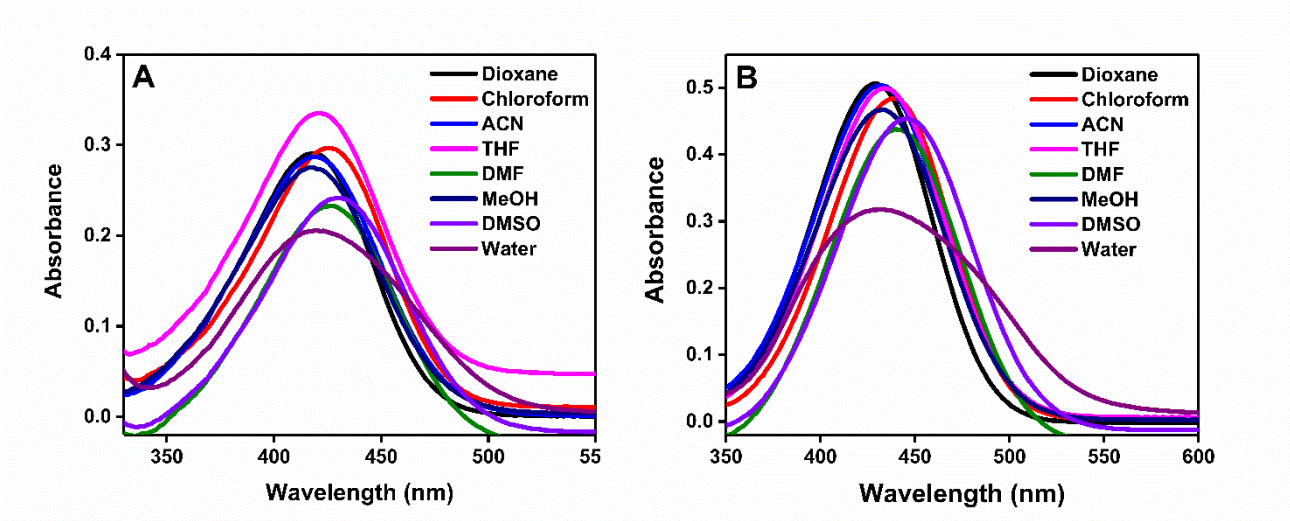

Fig. S1: The absorption spectrum of (A) PFN and (B) PFB [10 μM] in different solvents.

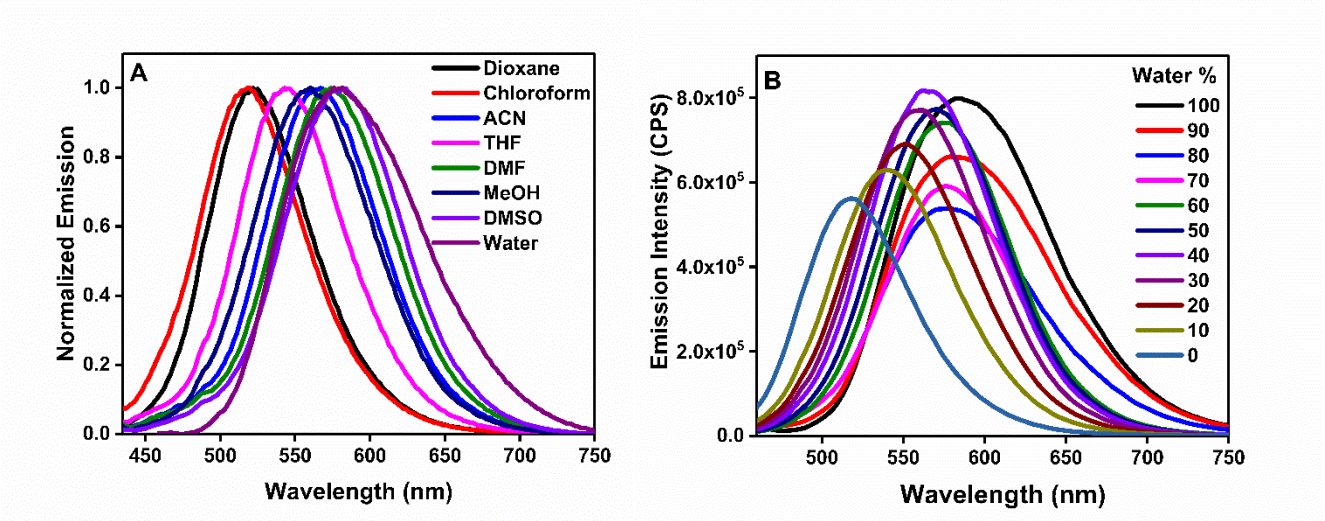

Fig S2: (A) The normalized emission spectra of PFN in different solvents. (B) Emission spectra of PFN in the dioxane/water binary solvent system. [Concentration = 15 μM.] The probe was excited at 425 nm for fluorescence experiments.

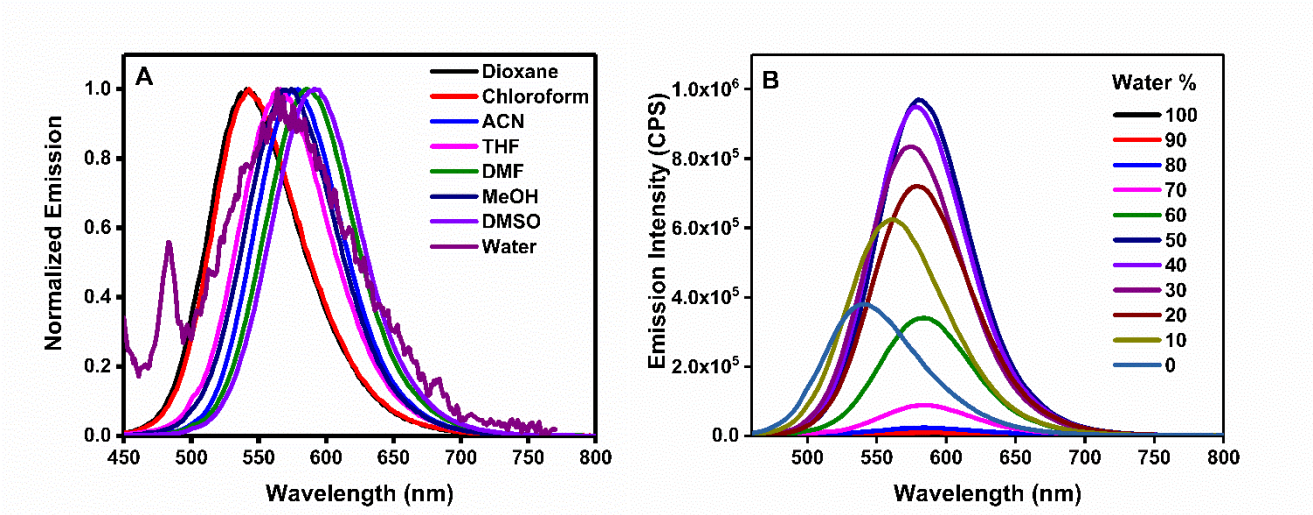

Fig S3: (A) The normalized emission spectra of PFB in different solvents. (B) Emission spectra of PFB in the dioxane/water binary solvent system. [Concentration = 15 μM.] The probe was excited at 435 nm for fluorescence experiments.

Fig S4. Dynamic Light Scattering (DLS) Spectra:

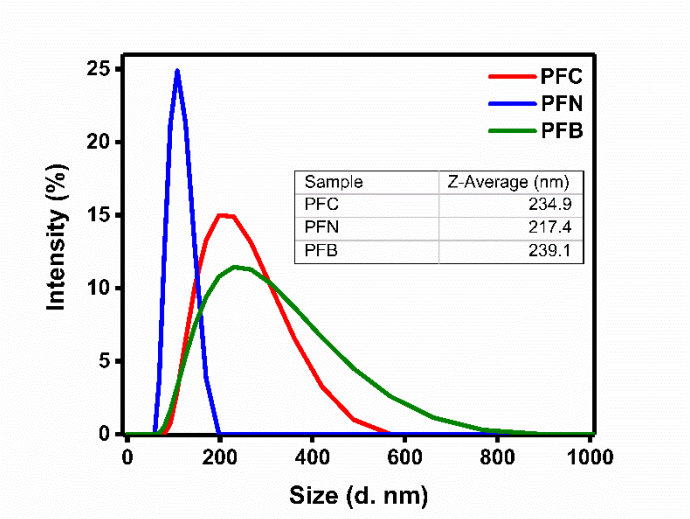

Fig S4: Dynamic Light Scattering Plots PFC, PFN, and PFB depicting size of aggregates formed in water. [Concentration-5 µM].

S4. Computational Details

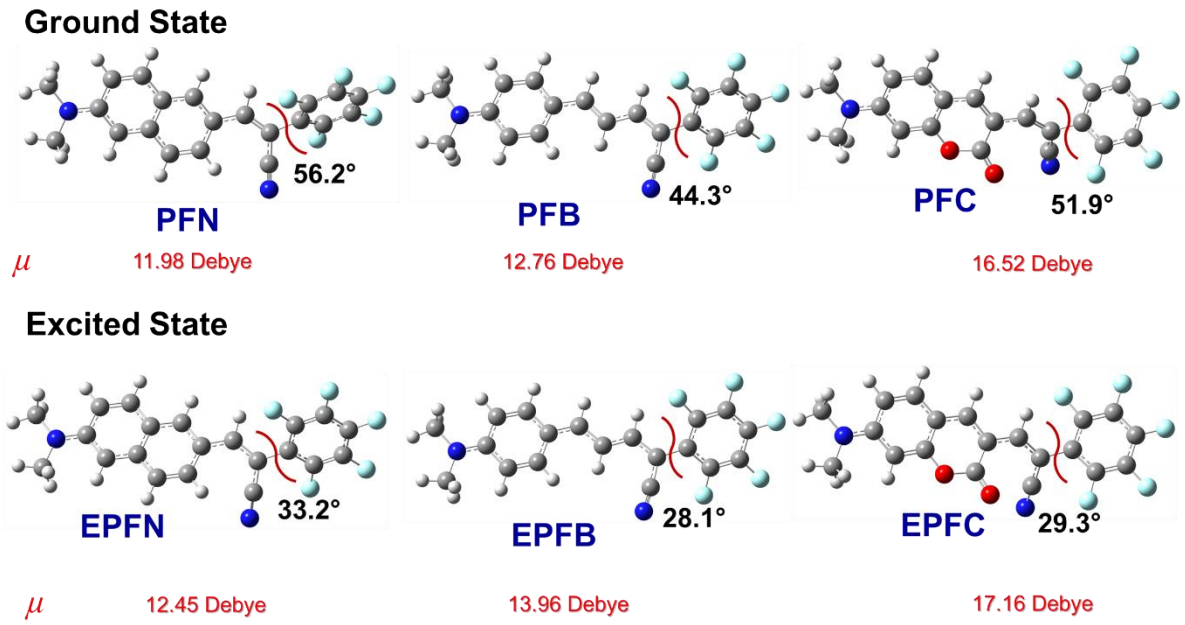

Fig S5. Optimized molecular geometries at the ground and excited states along with their dipole moment values and selected dihedral angles.

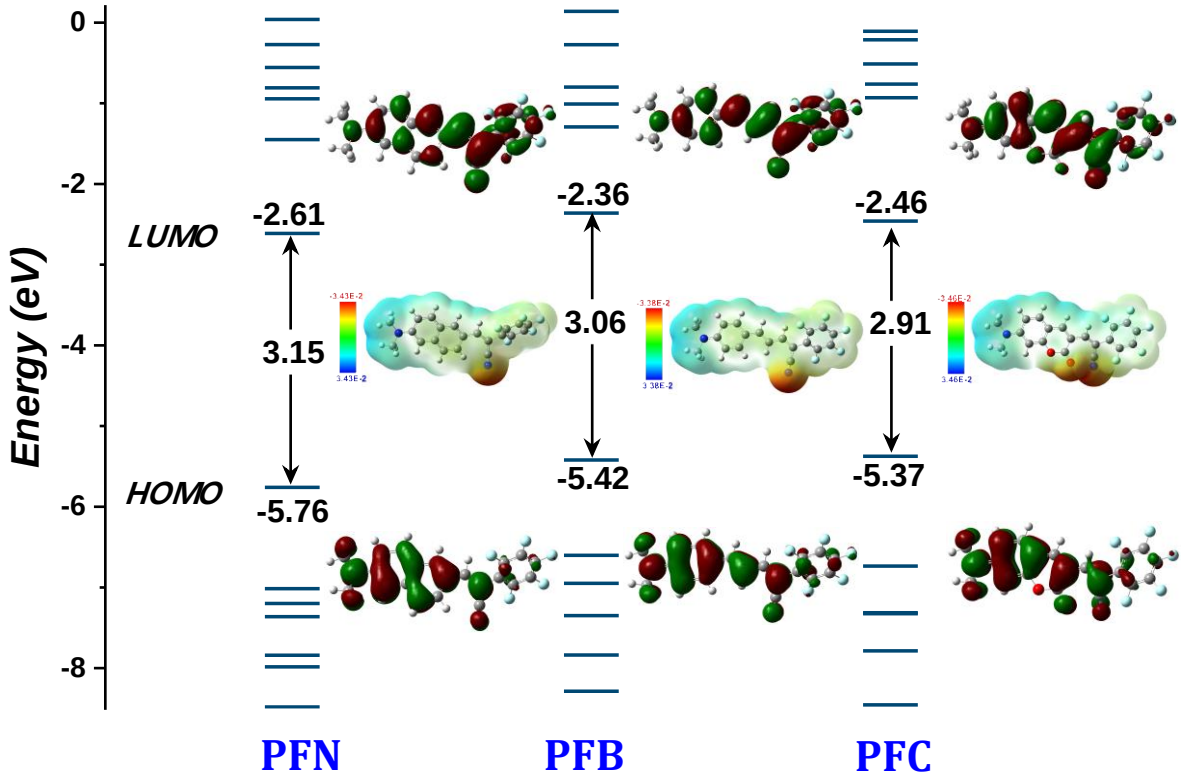

Fig S6. Schematic energy level diagram of the molecules investigated in this study and their isodensity surfaces corresponding to the frontier energy levels, electrostatic potential (ESP) surface plots.

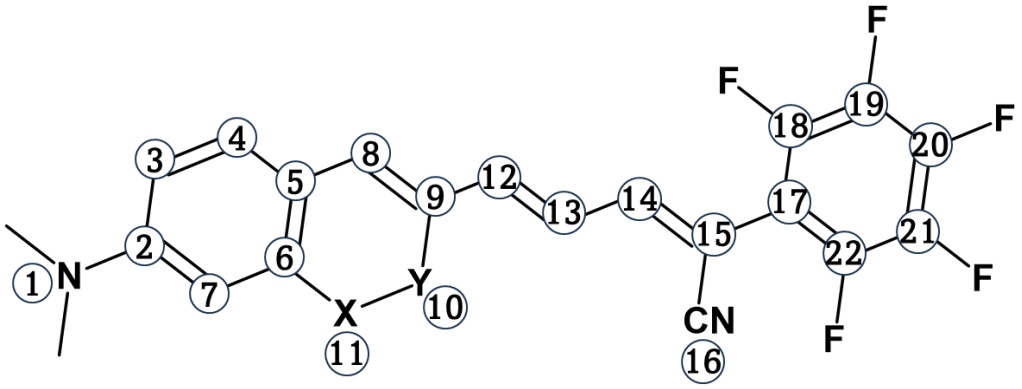

Å	PFN (GS)	PFN (ES)	PFB (GS)	PFB (ES)	PFC (GS)	PFC (ES)
N_1-C_2	1.369	1.368	1.365	1.365	1.359	1.364
C_2-C_3	1.403	1.432	1.423	1.425	1.417	1.431
C_3-C_4	1.405	1.368	1.378	1.376	1.379	1.373
C_4-C_5	1.433	1.431	1.413	1.426	1.412	1.421
C_5-C_6	1.421	1.430	1.411	1.423	1.415	1.419
C_6-C_7	1.367	1.405	1.380	1.375	1.371	1.377
C_7-C_2	1.436	1.415	1.419	1.426	1.432	1.420
C_5-C_8	1.428	1.402	-	-	1.409	1.412
C_8-C_9	1.367	1.416	-	-	1.380	1.408
C_9-Y_{10}	1.432	1.430	-	-	1.462	1.474
Y_{10}-X_{11}	1.396	1.371	-	-	1.394	1.391
X_{11}-C_6	1.405	1.426	-	-	1.365	1.368
$C_{5(9)}$-$C_{12\ (14)}$	1.445	1.440	1.440	1.432	1.446	1.421
C_{12}-C_{13}	-	-	1.364	1.392	-	-
C_{13}-C_{14}	-	-	1.422	1.402	-	-
C_{14}-C_{15}	1.364	1.407	1.372	1.417	1.359	1.404
C_{15}-C_{16}	1.424	1.417	1.424	1.418	1.427	1.419
C_{15}-C_{17}	1.488	1.459	1.480	1.450	1.491	1.464
C_{17}-C_{18}	1.398	1.415	1.400	1.418	1.397	1.413
C_{18}-C_{19}	1.387	1.384	1.387	1.381	1.387	1.384
C_{19}-C_{20}	1.389	1.390	1.388	1.392	1.389	1.390
C_{20}-C_{21}	1.388	1.391	1.388	1.390	1.388	1.391
C_{21}-C_{22}	1.388	1.382	1.387	1.383	1.388	1.383
C_{17}-C_{22}	1.398	1.415	1.400	1.418	1.397	1.413
Y_{10}=O	-	-	-	-	1.206	1.204

Fig S7. Geometrical coordinates of the molecules showing the bond length variation at the ground and excited states.

Fig S8. TDDFT simulated absorption spectra of the molecules obtained from the B3LYP, ωB97XD and M062X/6-311G(d, p)/C-PCM(1,4-dioxane) level of theory.

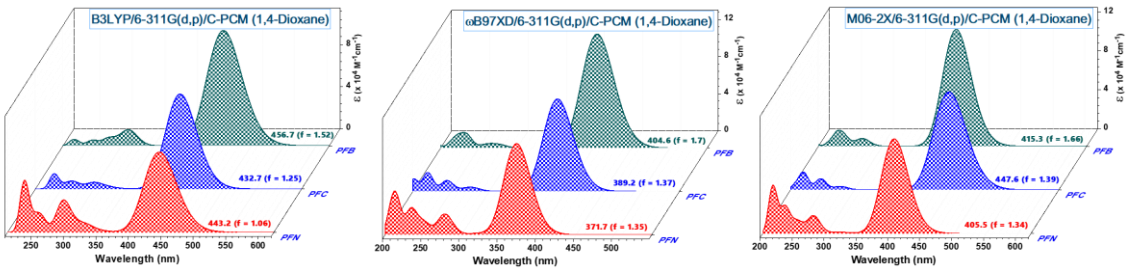

Table S1. TDDFT simulated spectral values, oscillator strength (f), and major transitions involved obtained from B3LYP/6-311G(d,p)/C-PCM(1,4-dioxane) level of theory.

B3LYP	States	λ_{Theory} (nm)	f	Major transitions involved
PFN	S_0-S_1	443.18	1.06	HOMO->LUMO (99%)
PFB	S_0-S_1	456.73	1.52	HOMO->LUMO (100%)
PFC	S_0-S_1	438.68	1.25	HOMO->LUMO (99%)

Table S2. TDDFT simulated spectral values, oscillator strength (f), and major transitions involved obtained from M062X/6-311G(d,p)/C-PCM(1,4-dioxane) level of theory.

M062X	States	λ_{Theory} (nm)	f	Major transitions involved
PFN	S_0-S_1	405.51	1.34	HOMO->LUMO (95%)
PFB	S_0-S_1	415.25	1.66	HOMO->LUMO (96%)
PFC	S_0-S_1	447.63	1.39	HOMO->LUMO (95%)

Table S3. TDDFT simulated spectral values, oscillator strength (f), and major transitions involved obtained from ωB97XD/6-311G(d,p)/C-PCM(1,4-dioxane) level of theory.

ωB97XD	States	λ_{Theory} (nm)	f	Major transitions involved
PFN	S_0-S_1	371.72	1.35	HOMO->LUMO (89%), H-2->LUMO (3%)
PFB	S_0-S_1	404.61	1.70	HOMO->LUMO (92%), H-1->LUMO (3%)
PFC	S_0-S_1	389.09	1.37	HOMO->LUMO (92%), H-1->LUMO (2%)

S5. Cytotoxicity Assessment

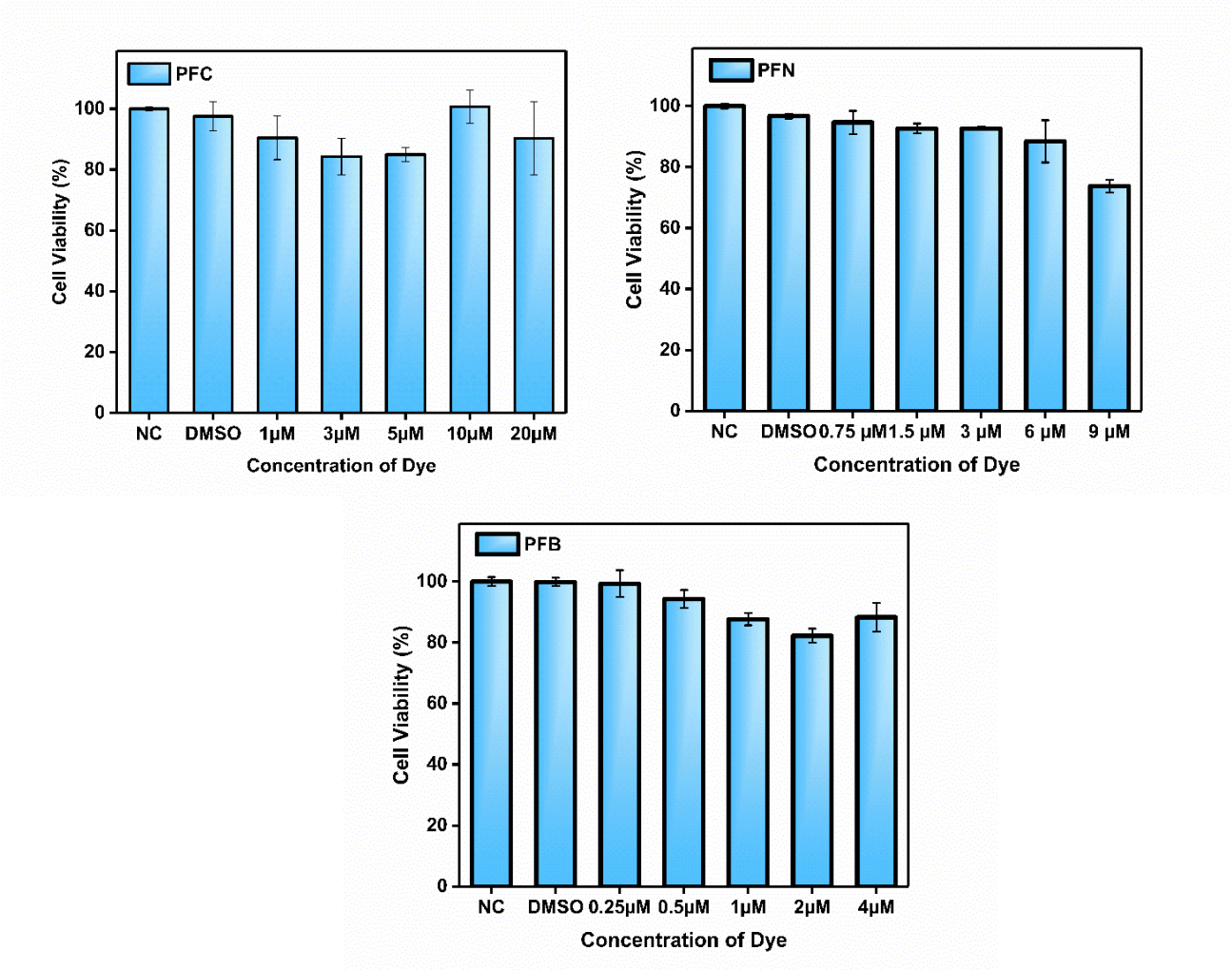

Fig S9: Cell viability data for PFC, PFN and PFB at various concentrations towards COS-7 cells for 24 h.

S6. Subcellular localization mapping of PFN and PFB in Live Cells

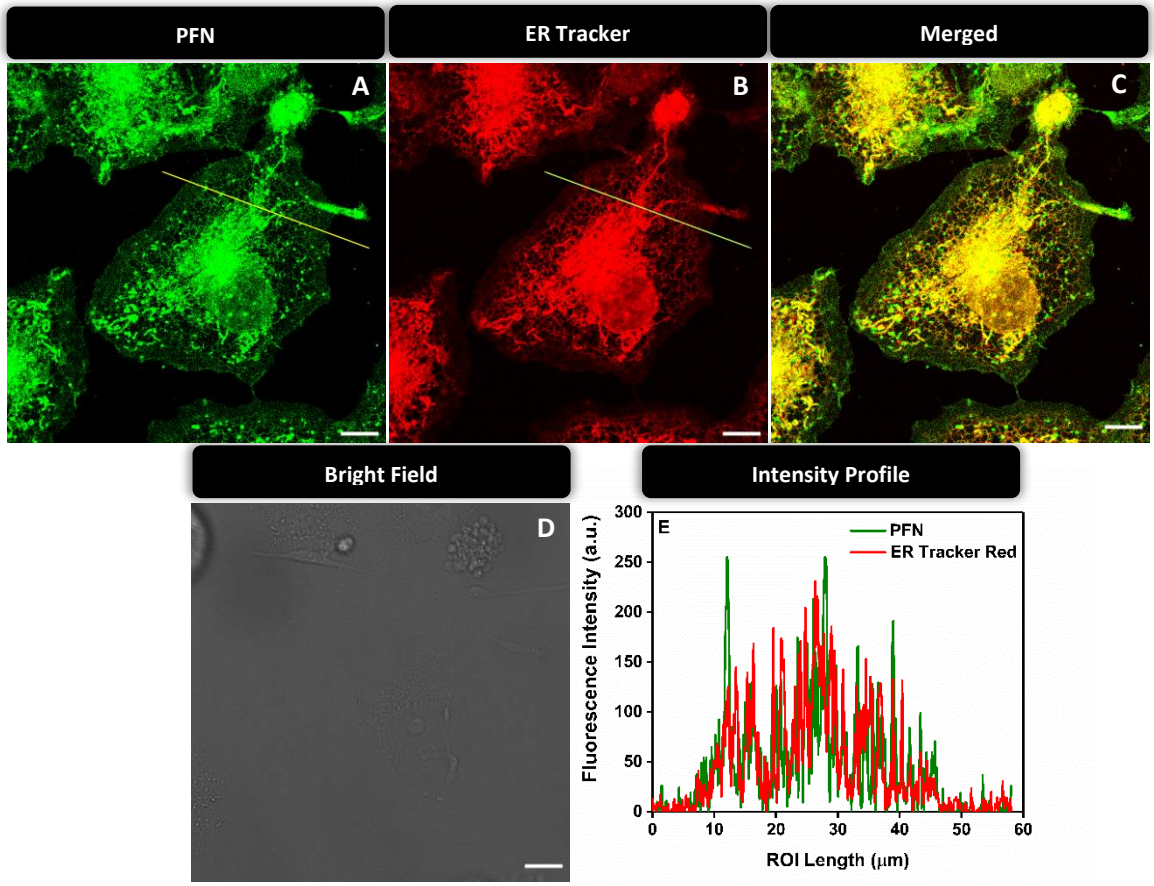

Fig S10: Fluorescence images of (A) PFN (3 μM) co-stained with (B) ER-Tracker™ Red in living COS-7 cell; Corresponding (C) Merged image, (D) Bright Field image; and (E) the intensity profile of the yellow lines drawn in both channels to describe the overlapping signal intensities. PFN: λ_{ex} = 488 nm (2%), λ_{em} = 500–620 nm; PCC = 0.82; Scale bar = 10 μm.

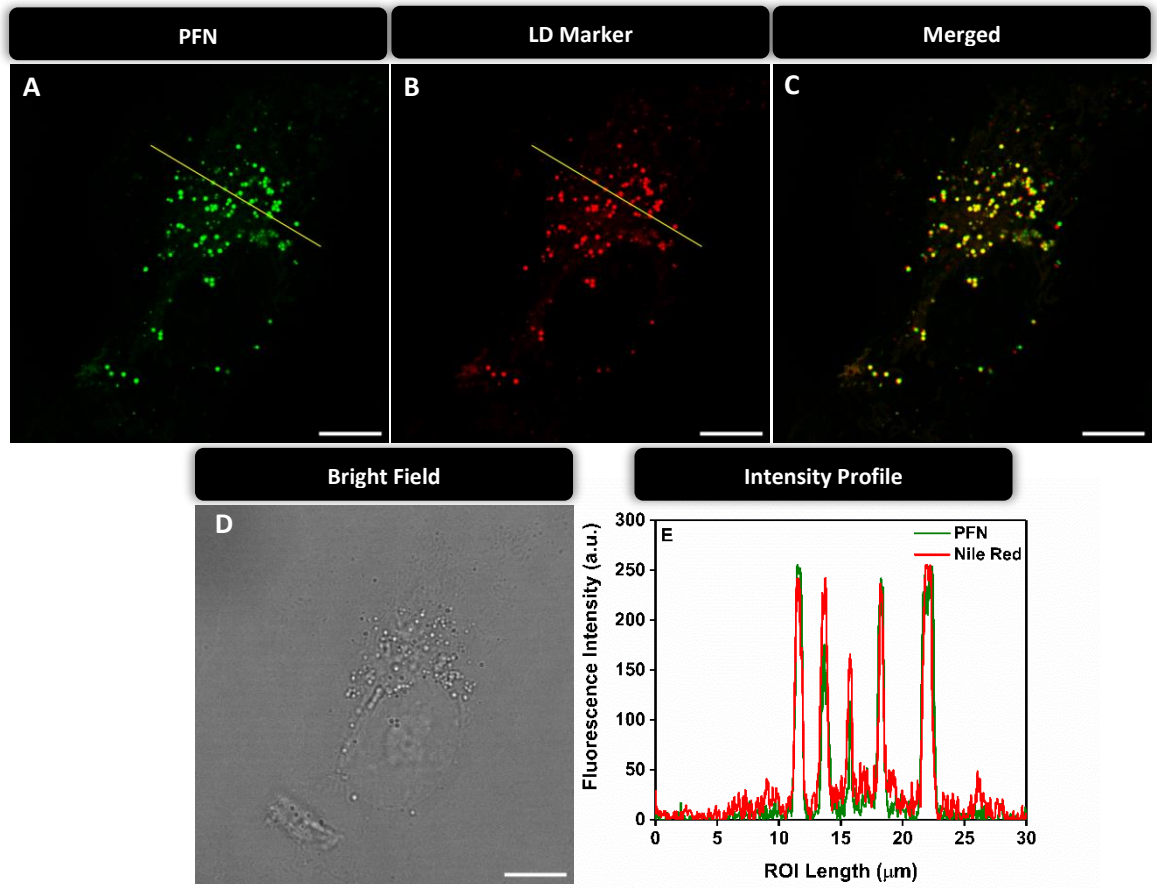

Fig S11: Fluorescence images of (A) PFN (3 μM) co-stained with (B) Nile Red in living COS-7 cell; Corresponding (C) Merged image, (D) Bright Field image; and (E) the intensity profile of the yellow lines drawn in both channels to describe the overlapping signal intensities. PFN: λ_{ex} = 488 nm (0.3 %), λ_{em} = 500–620 nm; PCC = 0.87; Scale bar = 10 μm.

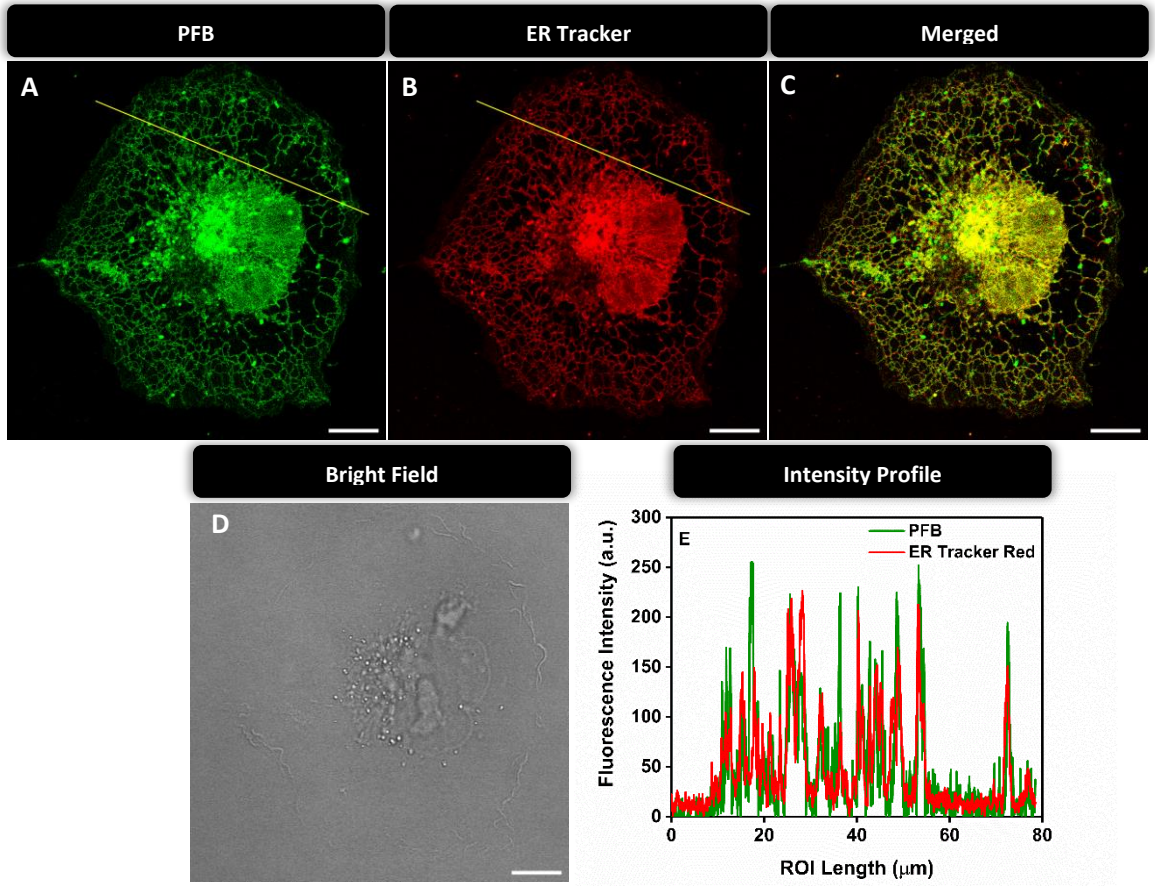

Fig S12: Fluorescence images of (A) PFB (3 μM) co-stained with (B) ER-Tracker™ Red in living COS-7 cell; Corresponding (C) Merged image, (D) Bright Field image; and (E) the intensity profile of the yellow lines drawn in both channels to describe the overlapping signal intensities. PFB: λ_{ex} = 488 nm (3 %), λ_{em} = 500–620 nm; PCC = 0.79; Scale bar = 10 μm.

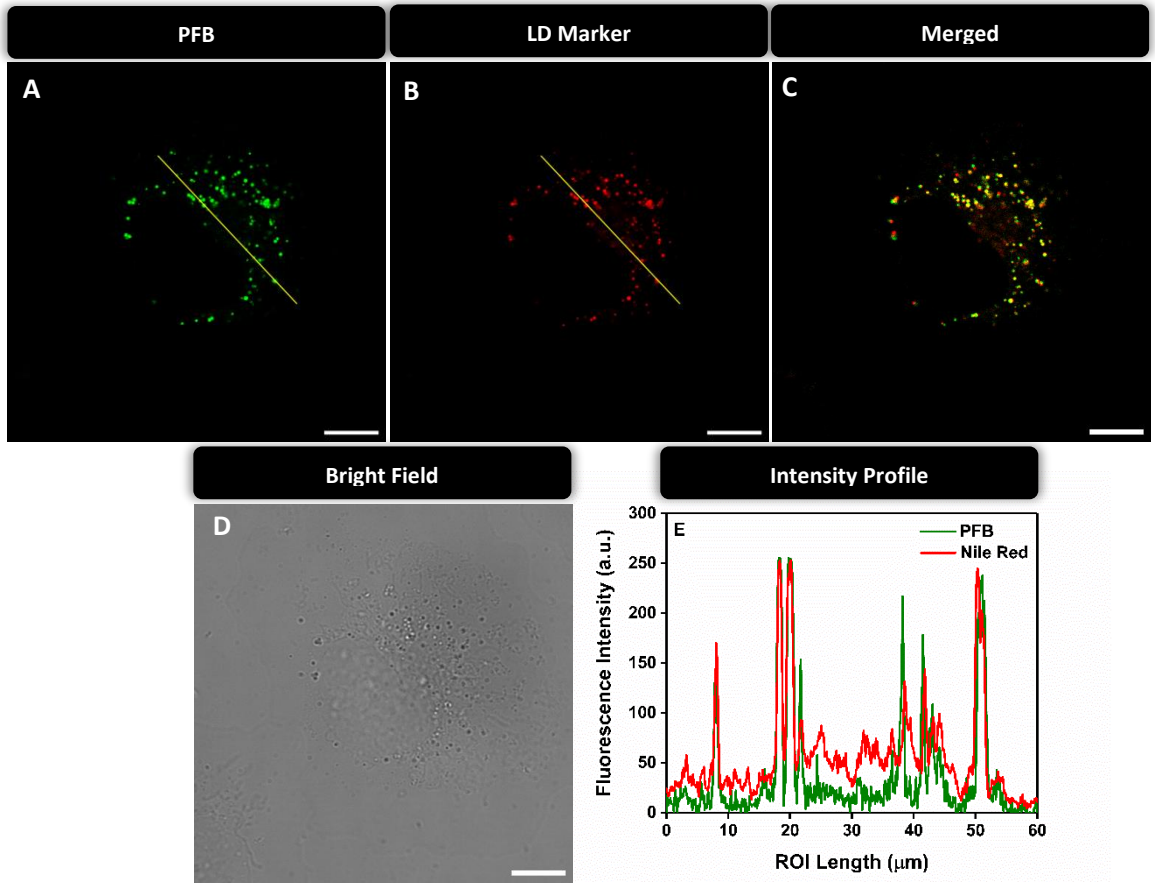

Fig S13: Fluorescence images of (A) PFB (3 μM) co-stained with (B) Nile Red in living COS-7 cell; Corresponding (C) Merged image, (D) Bright Field image; and (E) the intensity profile of the yellow lines drawn in both channels to describe the overlapping signal intensities. PFB: λ_{ex} = 488 nm (0.3 %), λ_{em} = 500–620 nm; PCC = 0.84; Scale bar = 10 μm

S7. Live MCF-7 Cell Imaging with PFC

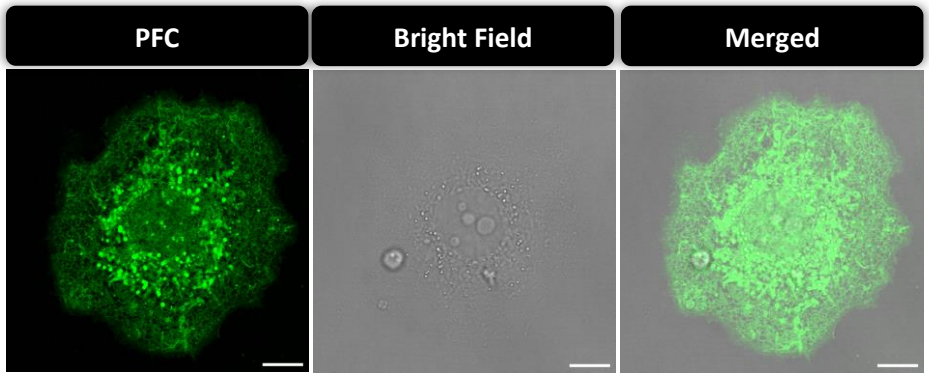

Fig S14: Fluorescence images of living MCF-7 cells stained with 100 nM PFC; λex = 488 nm, λem = 550–650 nm; Scale bar = 10 μm.

S8. Oleic acid treatment: CLSM images and quantification plots

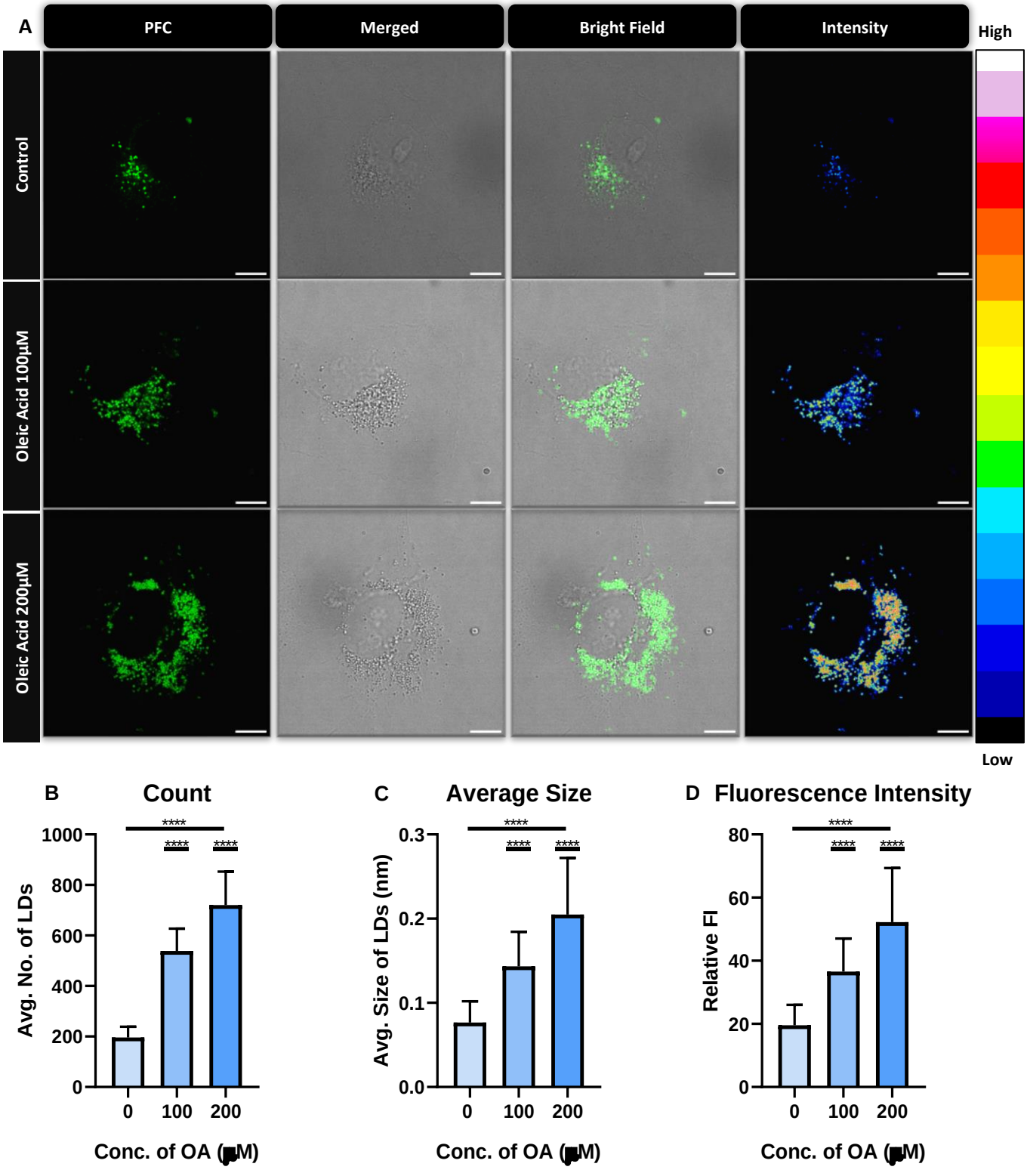

Fig S15: (A) CLSM images of PFC with incubation of 0 µM, 100 µM & 200 µM of oleic acid [scale bar: 10 µm]. (0. 3% Laser Power) Quantification plots for oleic acid accumulation: (B) quantification of change in number; (C) change in size (mean diameter); (D) and fluorescence intensity of lipid droplets.

S9. Photostability assessment of PFC in Live Cells

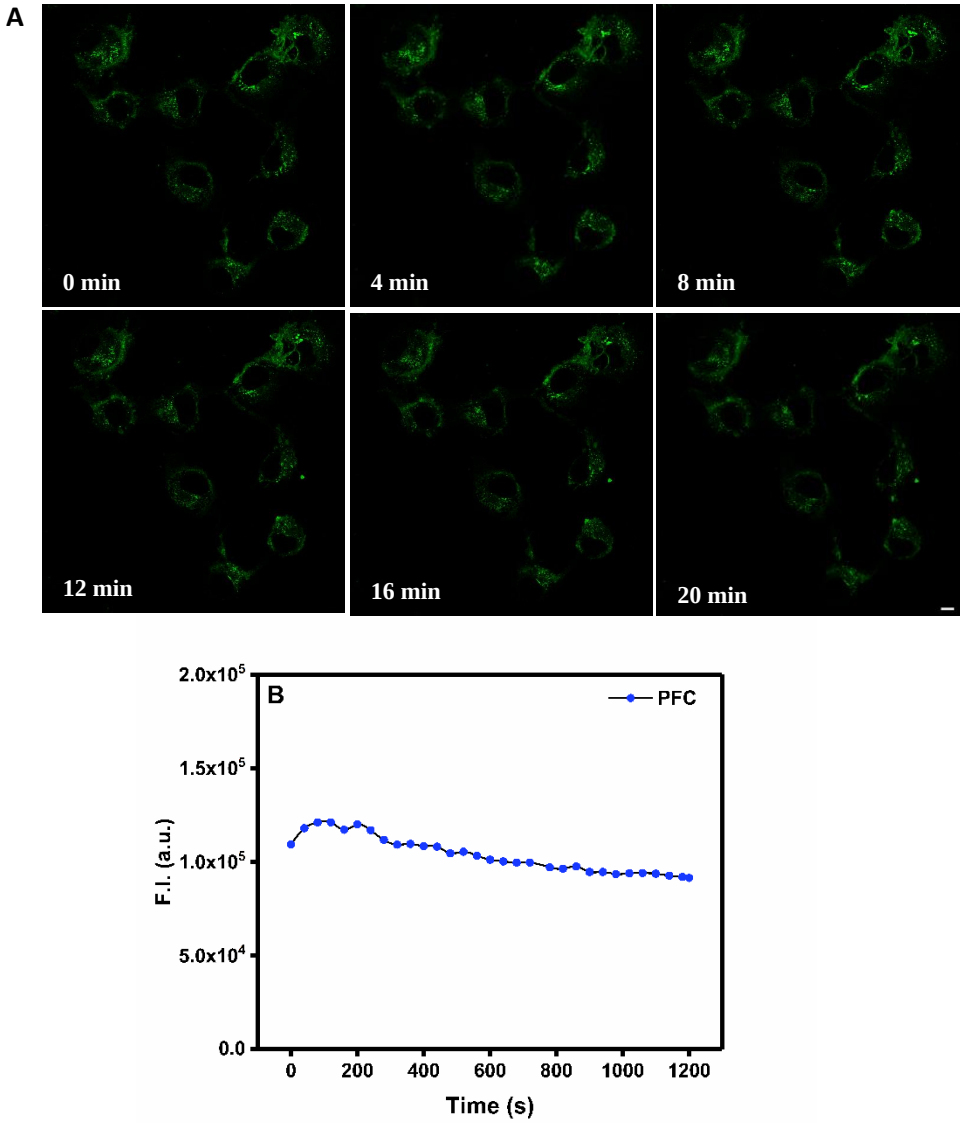

Fig S16: Fluorescent images (A) of COS-7 cells stained with PFC under continuous light irradiations and (B) the corresponding fluorescence intensity. Scale Bar = 10µm

S10. Characterization: NMR and HRMS Data for All Compounds

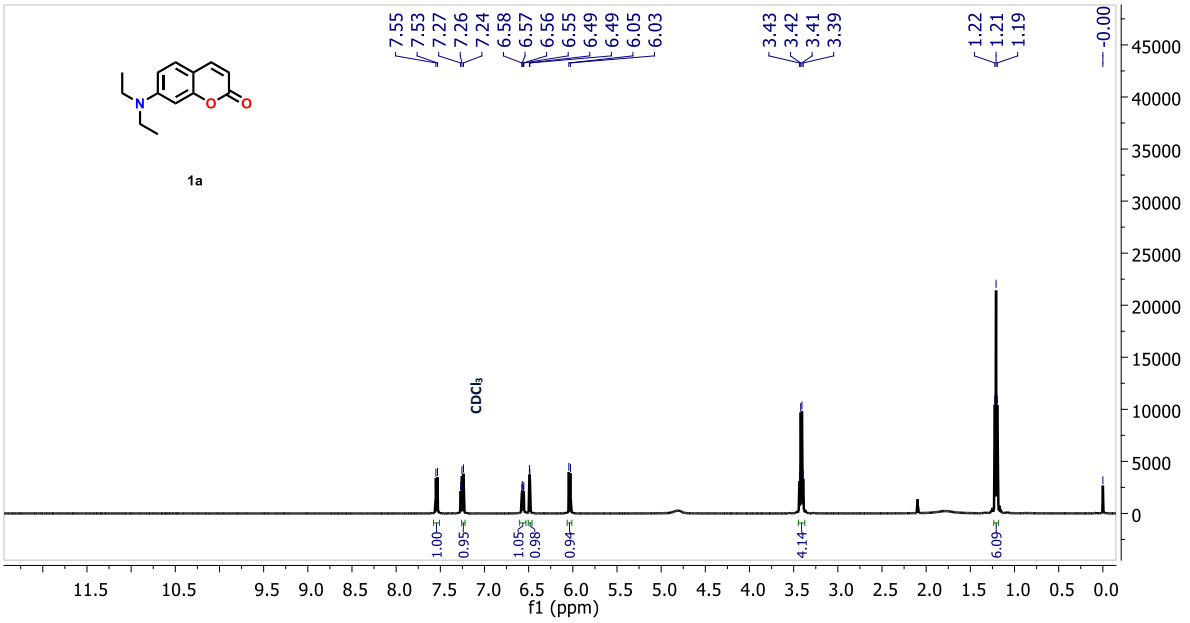

*Fig S17: ^{1}H Spectrum of **1a** in $CDCl_3$*

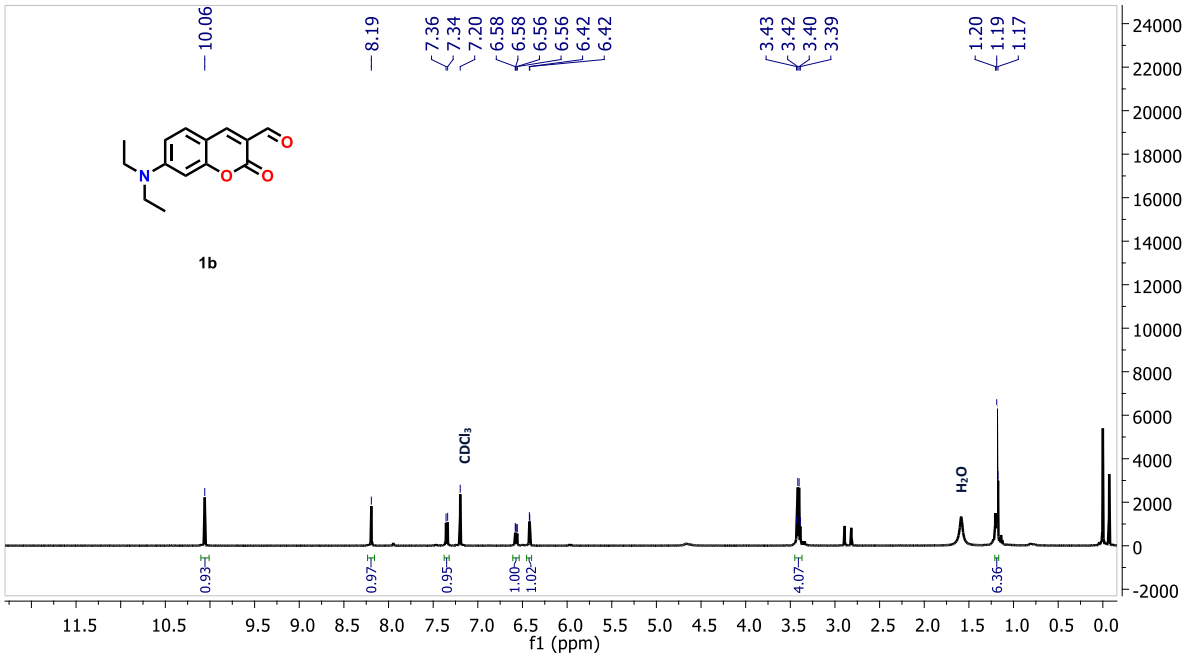

*Fig S18: ^{1}H Spectrum of **1b** in $CDCl_3$*

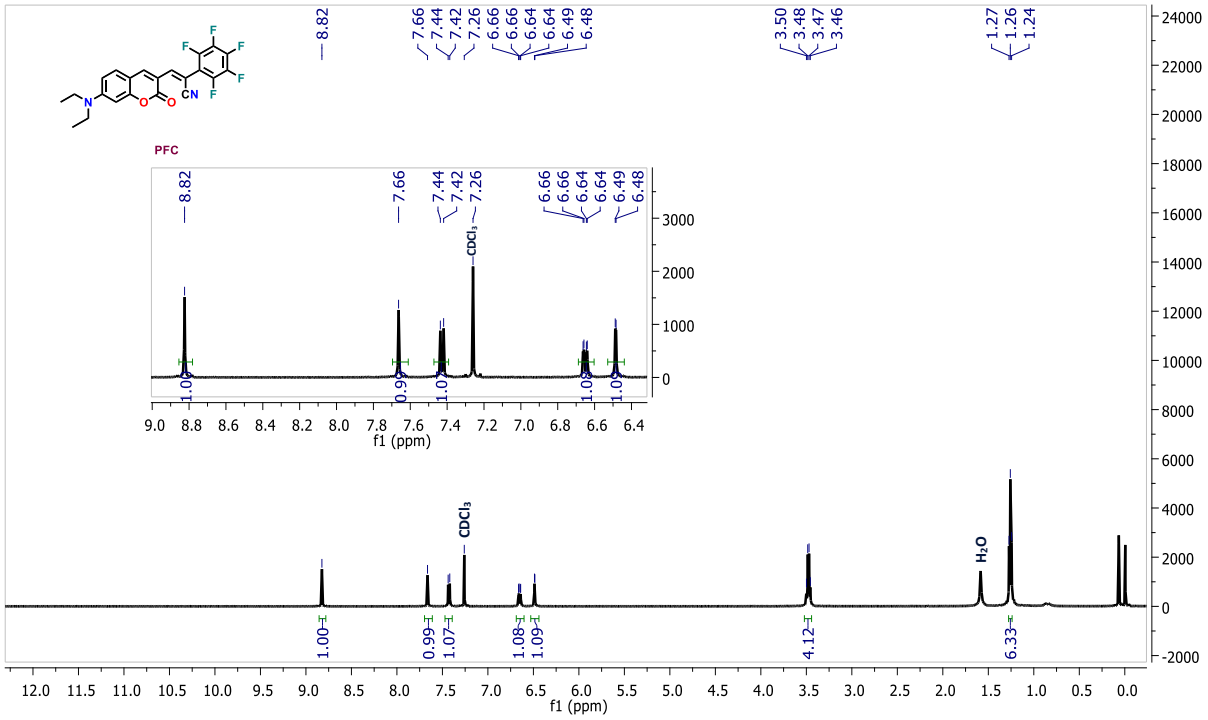

Fig S19: ^{1}H Spectrum of PFC in $CDCl_3$

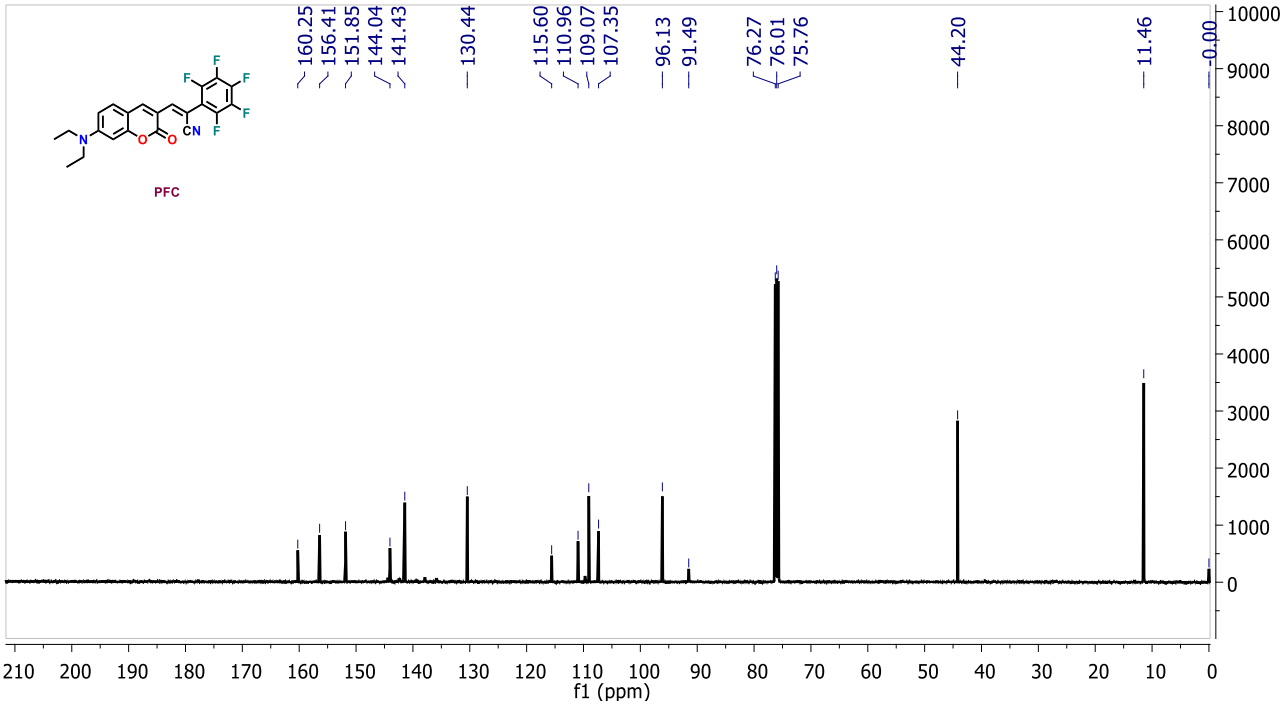

Fig S20: ^{13}C Spectrum of PFC in $CDCl_3$

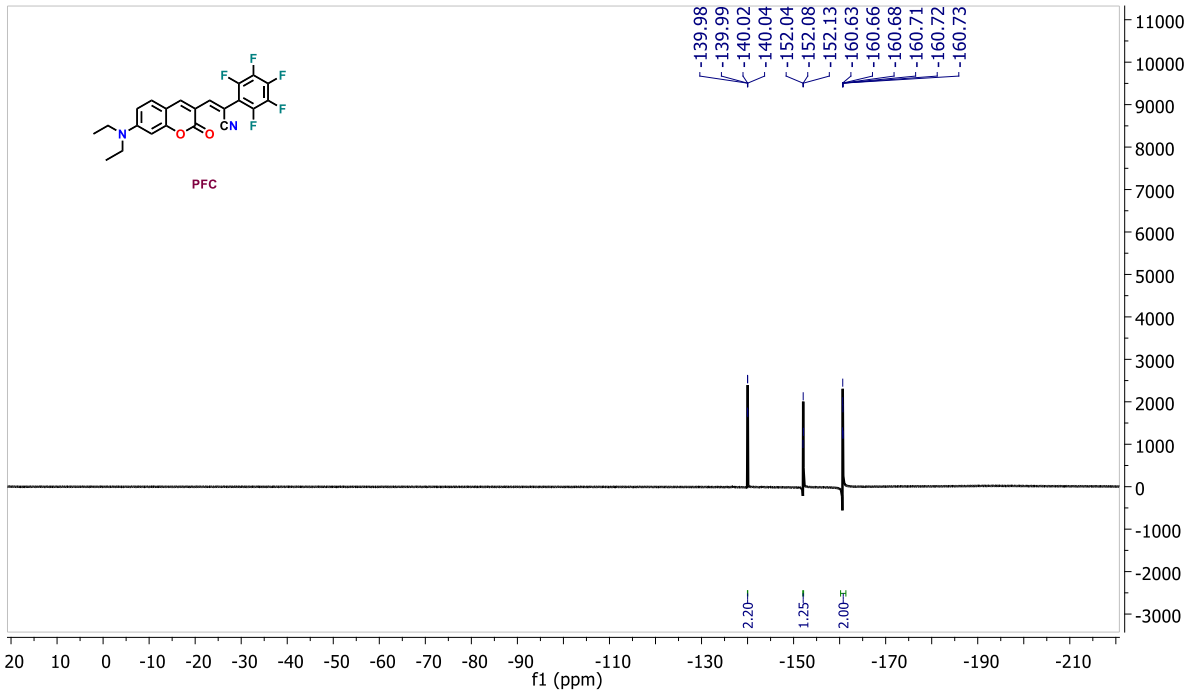

Fig S21: ^{19}F Spectrum of PFC in $CDCl_3$

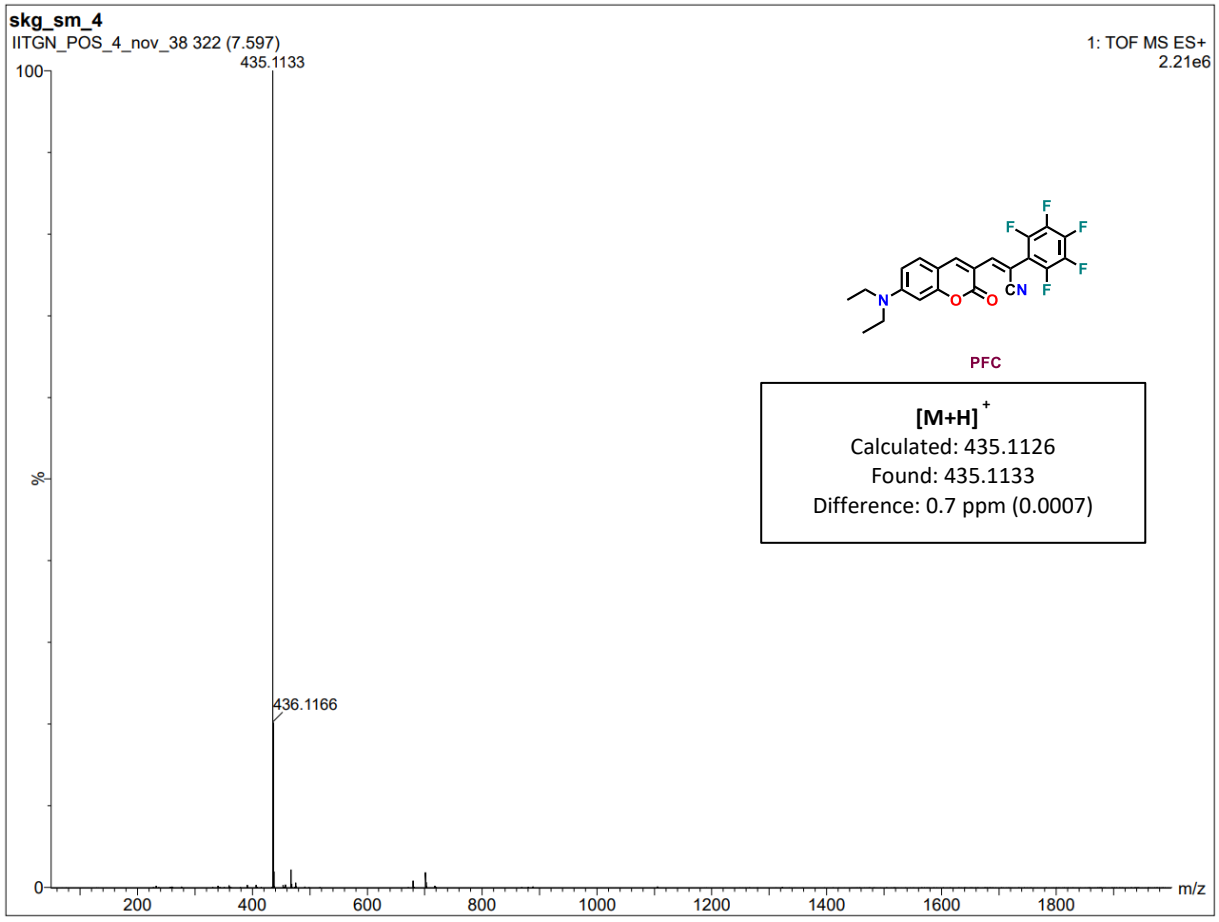

Fig S22: ESI mass profile of PFC

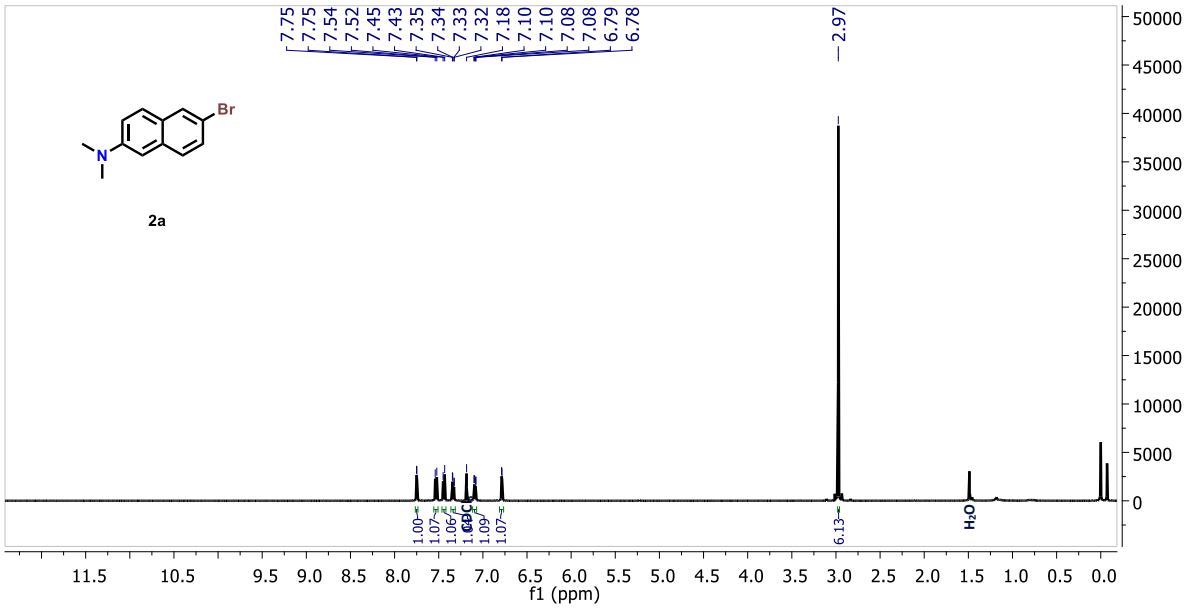

*Fig S23: 1H Spectrum of **2a** in $CDCl_3$*

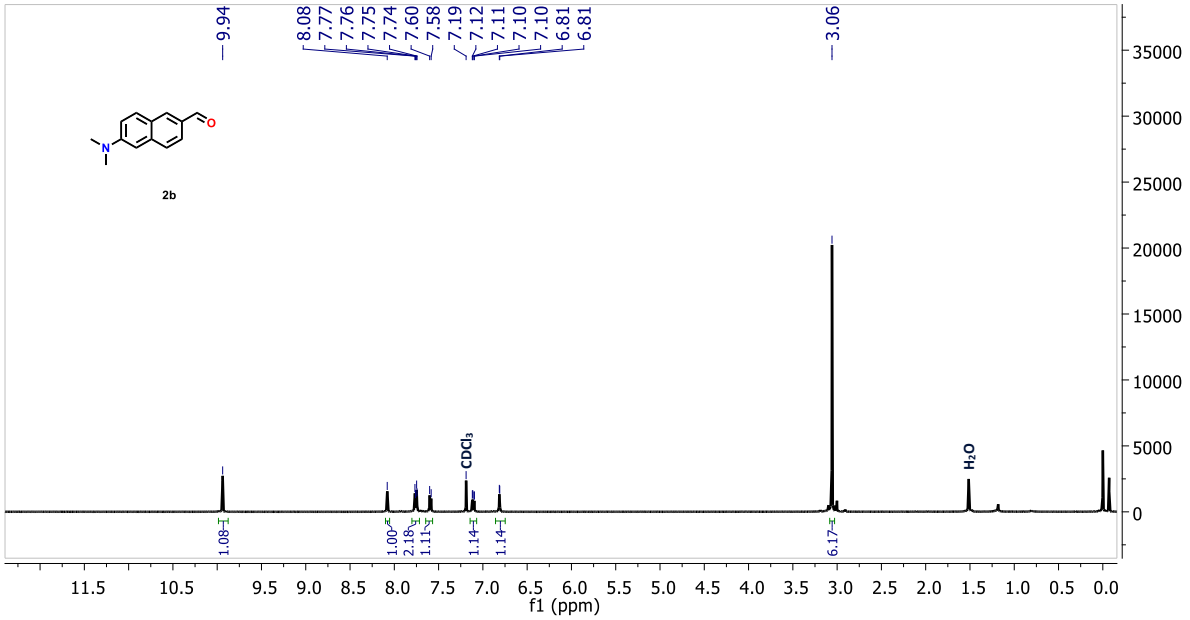

*Fig S24: ^1H Spectrum of **2b** in $CDCl_3$*

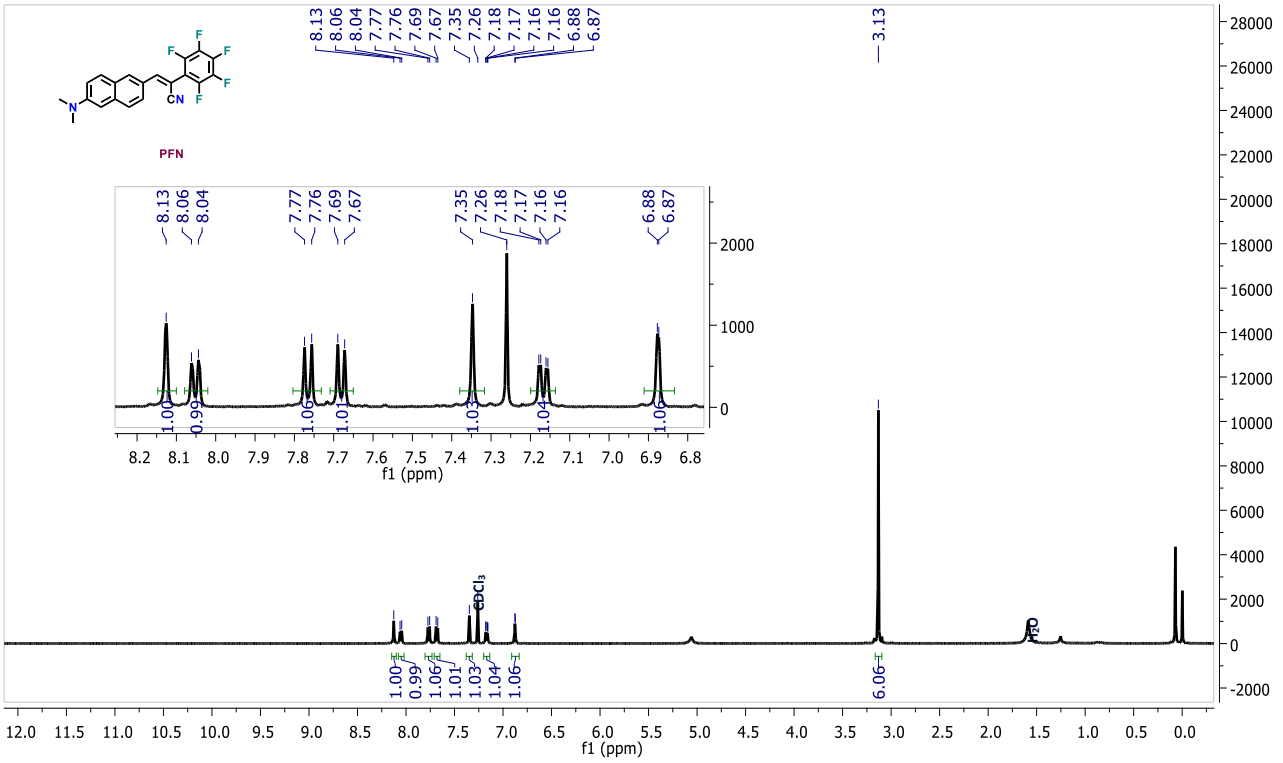

Fig S25: ^{1}H Spectrum of PFN in $CDCl_3$

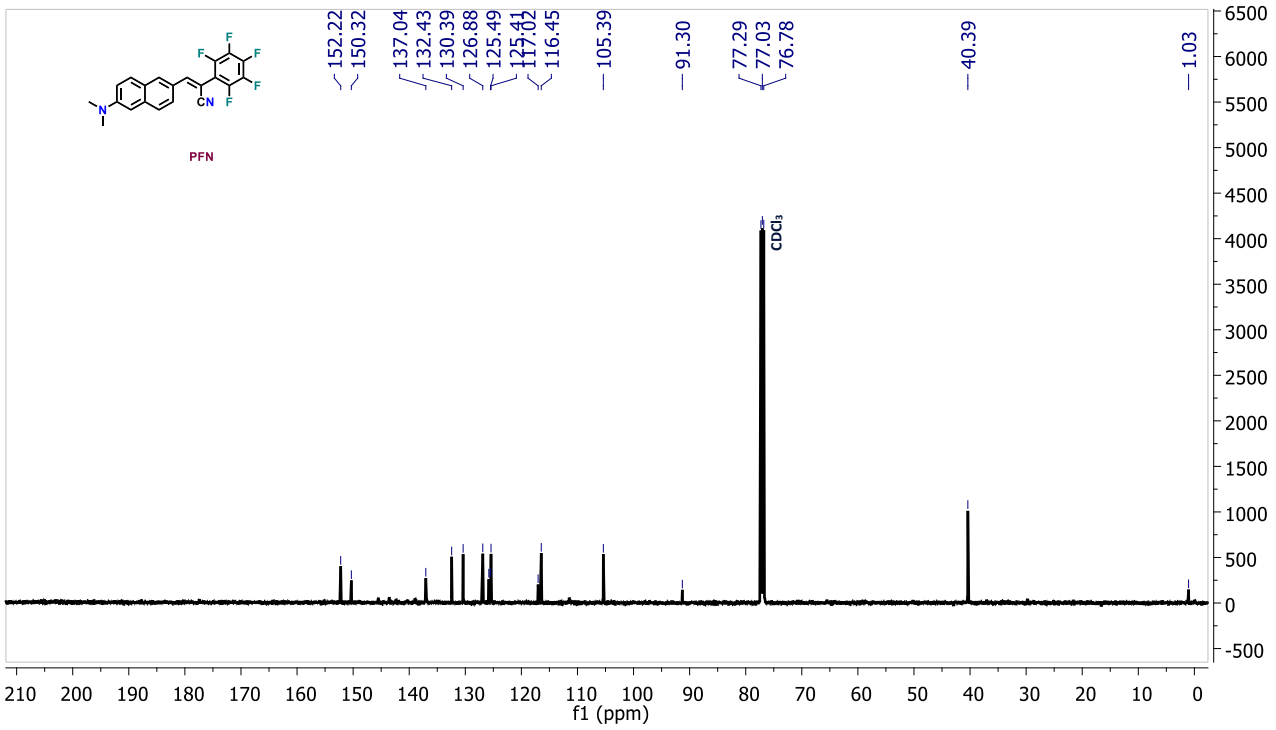

Fig S26: ^{13}C Spectrum of PFN in $CDCl_3$

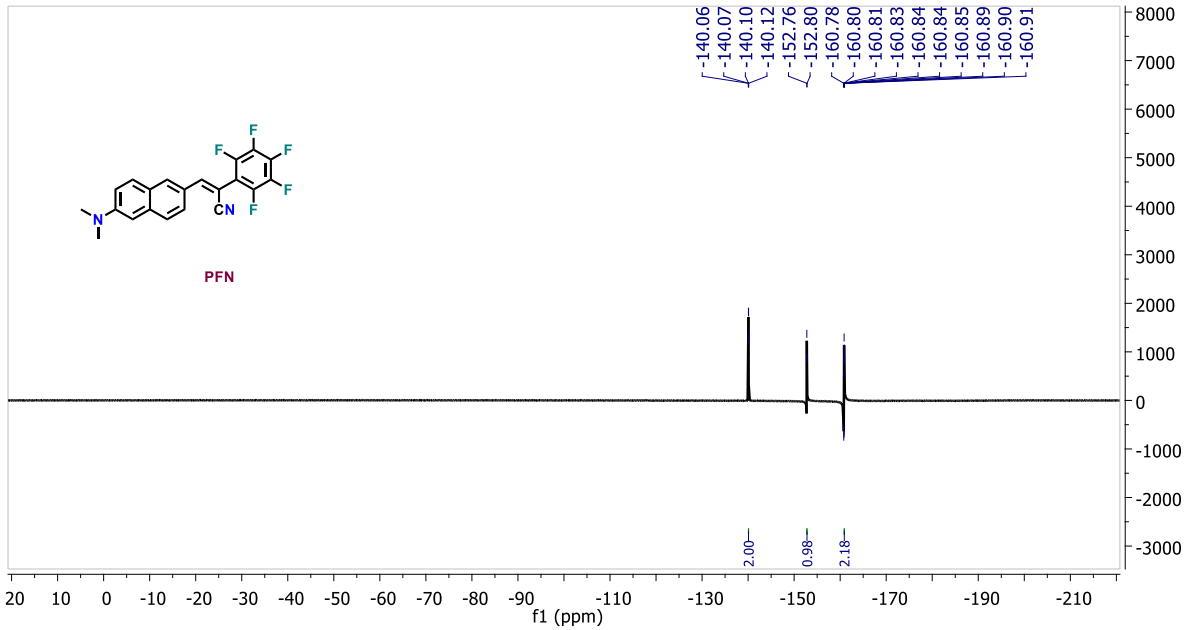

Fig S27: ^{19}F Spectrum of PFN in $CDCl_3$

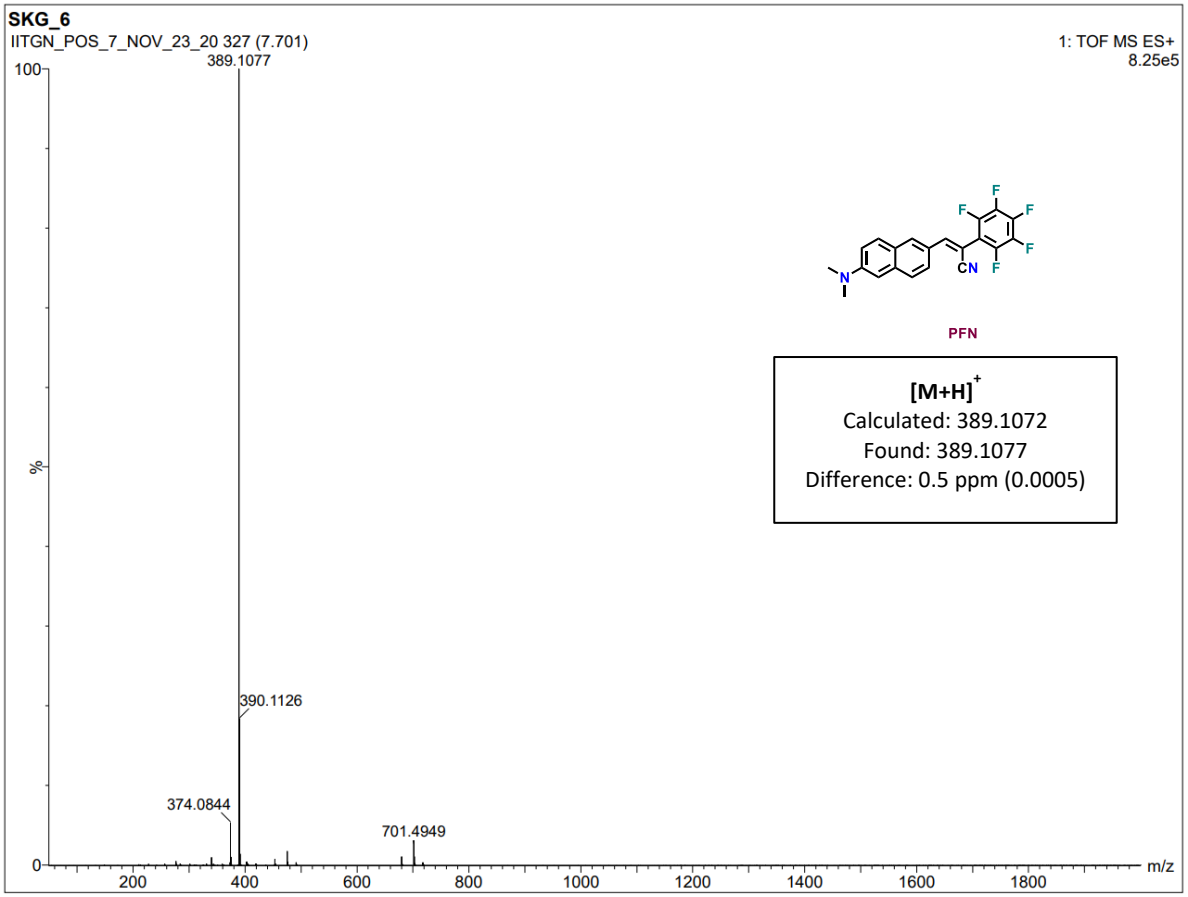

Fig S28: ESI mass profile of PFN

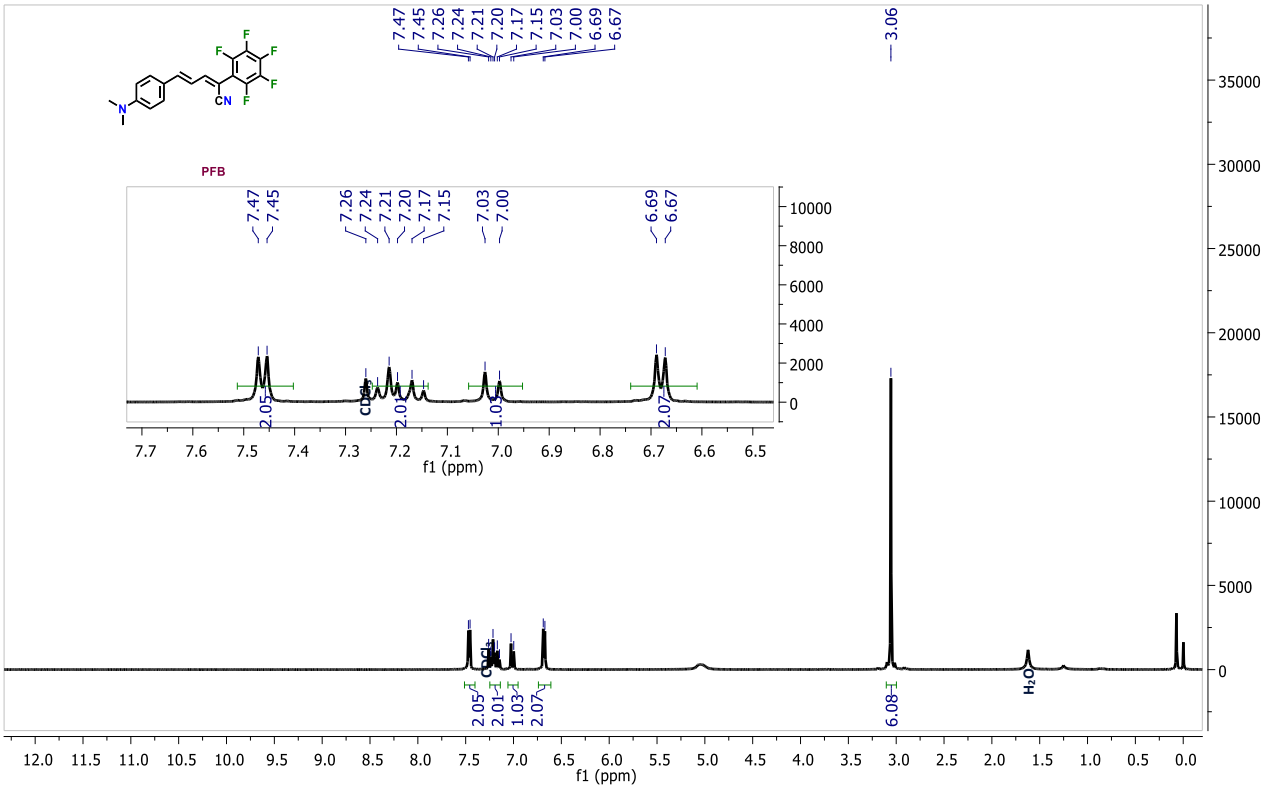

Fig S29: ^{1}H Spectrum of PFB in $CDCl_3$

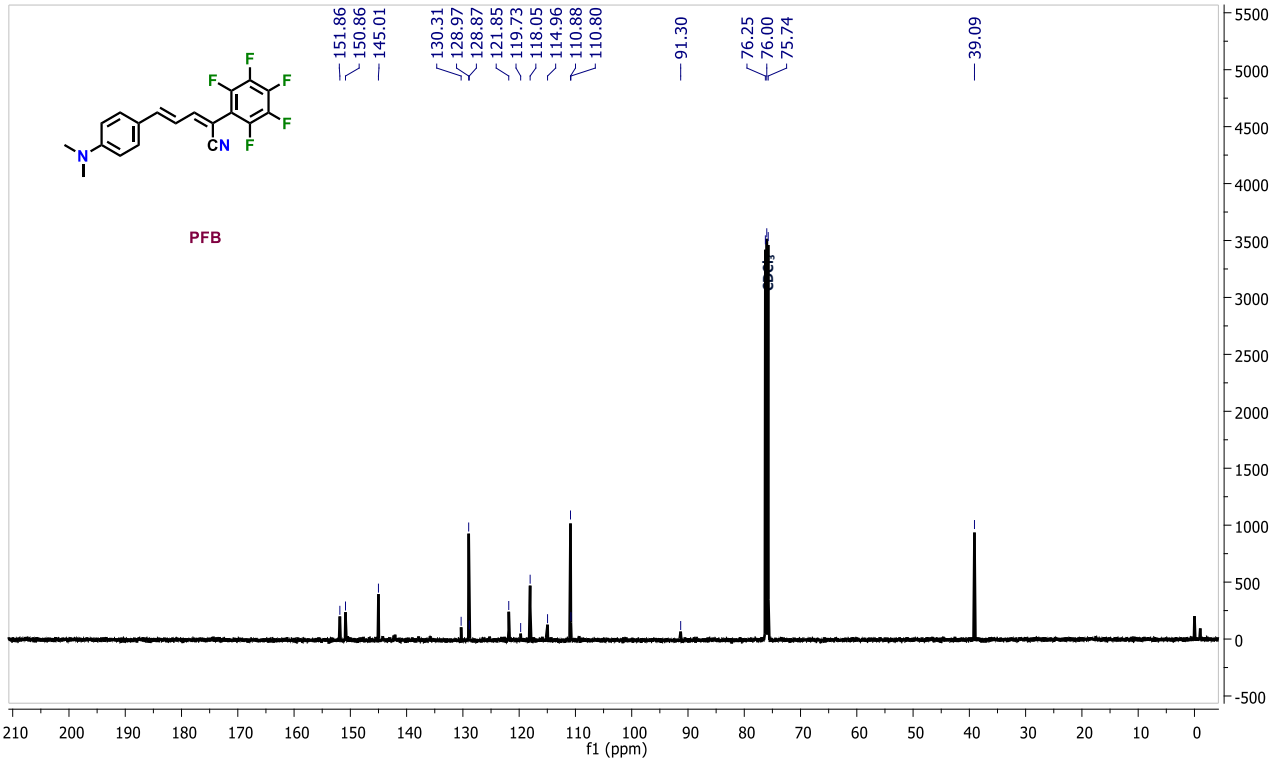

Fig S30: ^{13}C Spectrum of PFB in $CDCl_3$

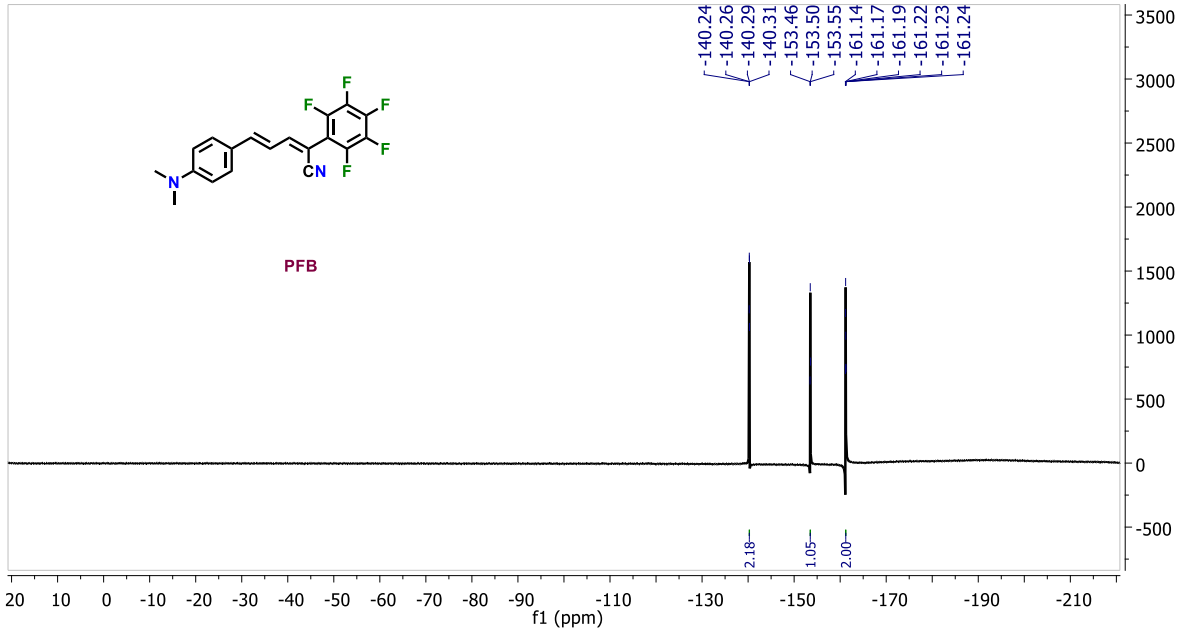

Fig S31: ^{19}F Spectrum of PFB in $CDCl_3$

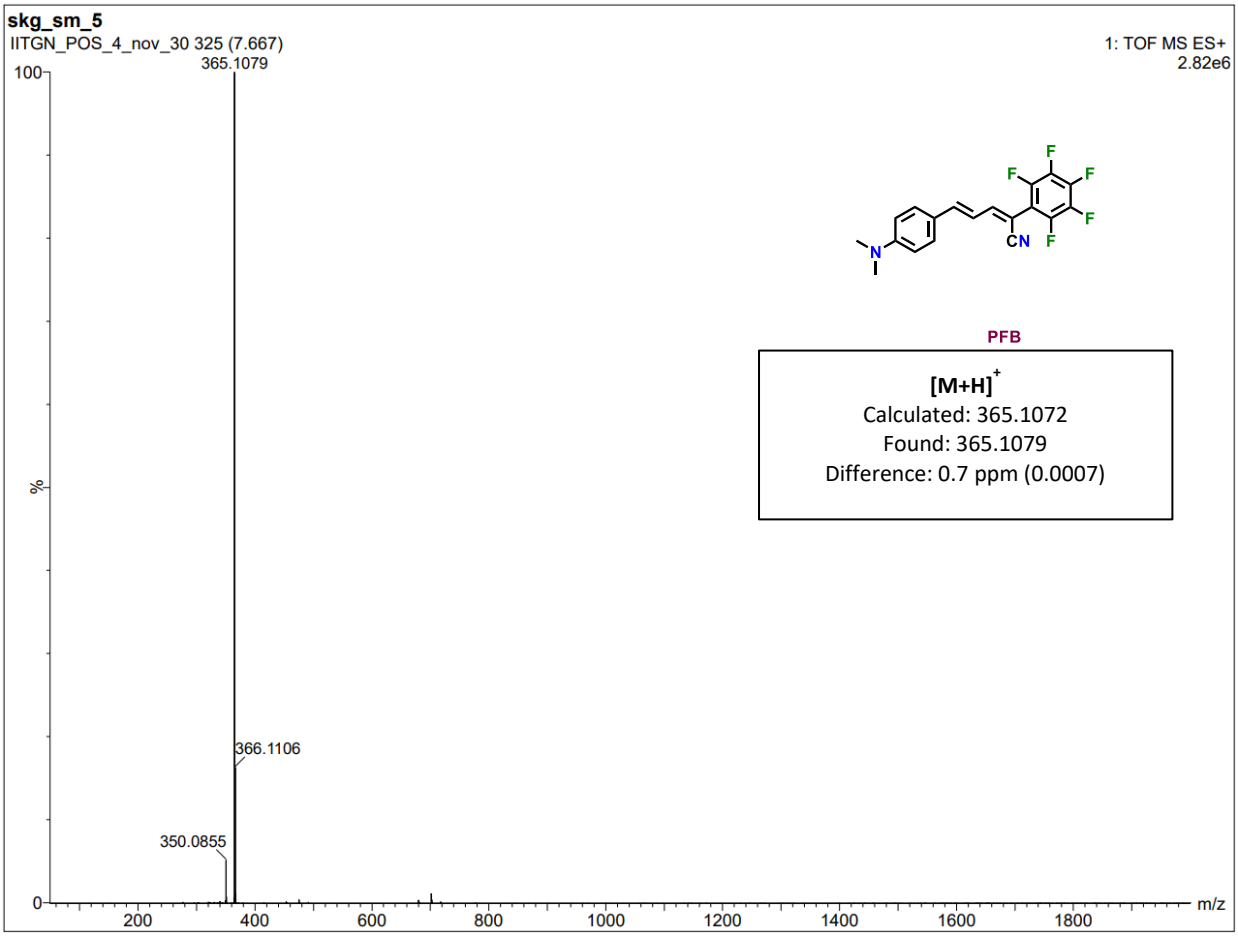

Fig S32: ESI mass profile of PFB

S11. References

(1) Wang, Y.; Li, Y.; Yu, T.; Su, W.; Ma, H.; Zhao, Y.; Li, X.; Zhang, H. Functionalized coumarin derivatives containing aromatic-imidazole unit as organic luminescent materials. *Dyes and Pigments* **2020**, *173*, 107958. DOI: https://doi.org/10.1016/j.dyepig.2019.107958.
(2) Rao, A. S.; Kim, D.; Wang, T.; Kim, K. H.; Hwang, S.; Ahn, K. H. Reaction-Based Two-Photon Probes for Mercury Ions: Fluorescence Imaging with Dual Optical Windows. *Org. Lett.* **2012**, *14* (10), 2598-2601. DOI: 10.1021/ol3009057.